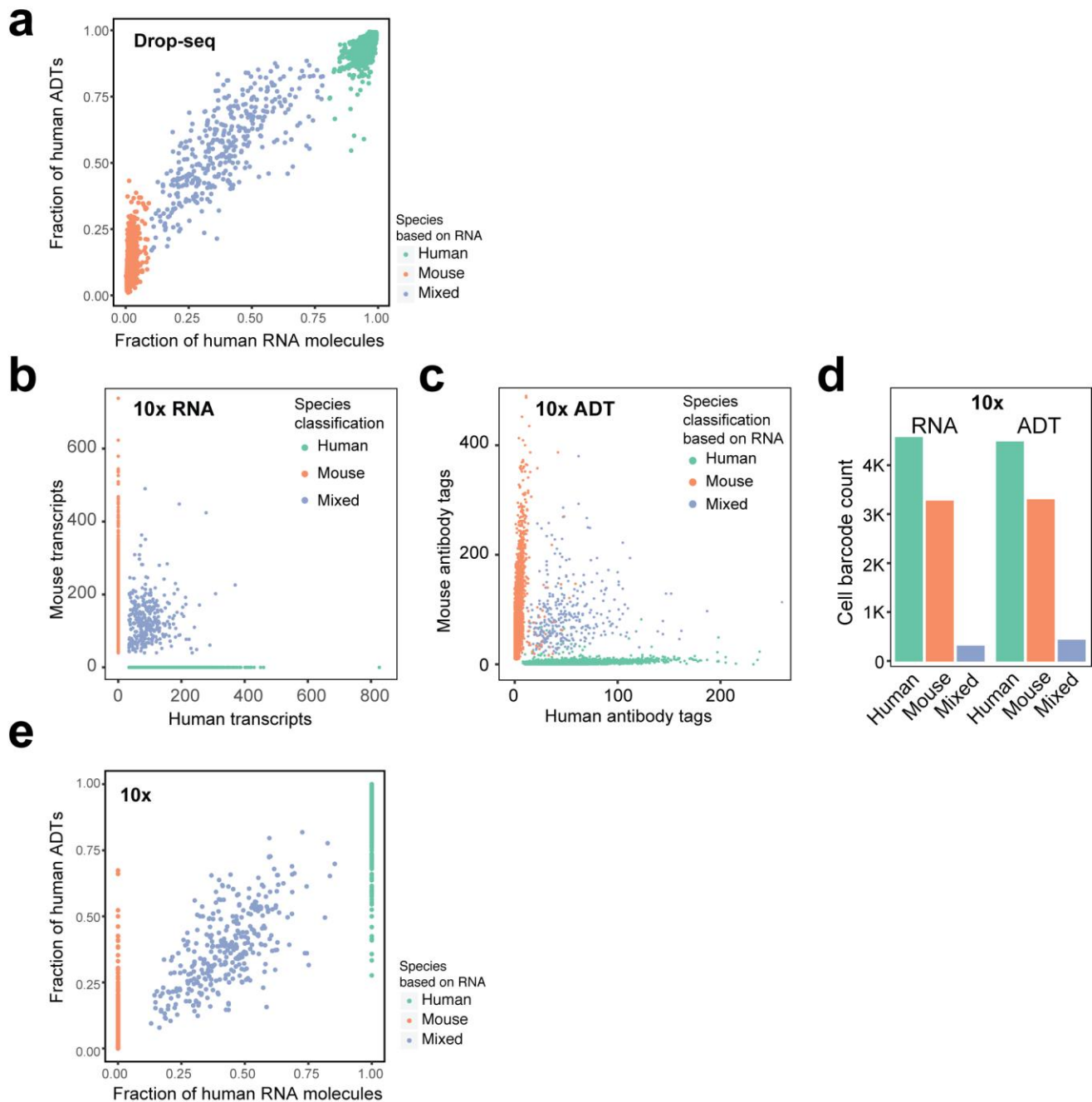**Supplementary Figure 1**

CITE-seq library preparation.

(**a**) Illustration of the DNA-barcoded antibodies used in CITE-seq. (**b**) Antibody-oligonucleotide complexes appear as a high-molecular-weight smear when run on an agarose gel (1). Cleavage of the oligo from the antibody by reduction of the disulfide bond collapses the smear to oligo length (2). (**c**) Drop-seq beads are microparticles with conjugated oligonucleotides comprising a common PCR handle, a cell barcode, followed by a unique molecular identifier (UMI) and a polyT tail[1]. (**d**) Schematic illustration of CITE-seq library prep in Drop-seq[1] (downstream of Fig. 1b). Reverse transcription and template switch is performed in bulk after emulsion breakage. After amplification, full length cDNA and antibody-oligo products can be separated by size and amplified independently (also shown in d) (**e**) Reverse transcription and amplification produces two product populations with distinct sizes (left panel). These can be size separated and amplified independently to obtain full length cDNAs (top panel, capillary electrophoresis trace) and ADTs (bottom panel, capillary electrophoresis trace).
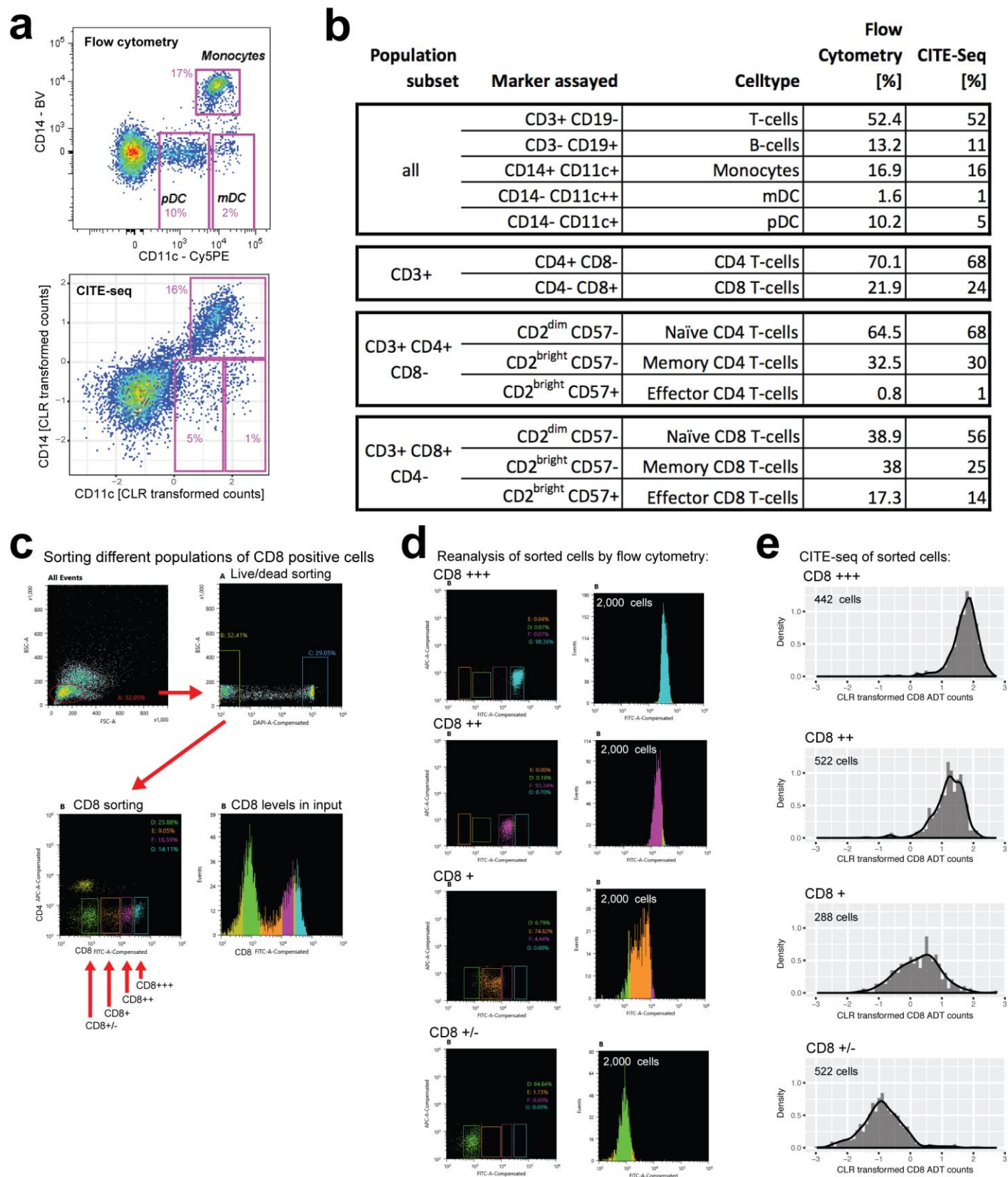
Supplementary Figure 2

Analysis of mixtures of mouse and human cells that were incubated with oligo-tagged-antibodies specific for either human or mouse cell-surface markers.

(a) Fractions of human RNA molecules compared to human ADTs for detected cell barcodes in the Drop-seq species mixing experiment. Each point represents one cell barcode (*i.e.,* droplet containing one or more cells). (**b-e**) CITE-seq of human and mouse mixing experiment repeated on a commercially available system from 10x Genomics. (**b**) Quantification of the number of human and mouse transcripts associating to each cell barcode. Each green point indicates a cell barcode (i.e. droplet containing one or more cells) from which we measured >90% human transcripts; each red point indicates a cell barcode with >90% mouse transcripts. Blue

points indicate cell barcodes (i.e. droplets) from which we observed a mixture of human and mouse transcripts. (**c**) Quantification of antibody tags (ADTs) associated with each cell barcode. Points are colored based on species classifications using transcripts in panel b. (**d**) Quantification of human, mouse or mixed-cell barcodes based on RNA transcripts, or ADTs, detected in 10x Genomics workflows. **(e)** Fractions of human RNA molecules compared to human ADTs for detected cell barcodes. Each point represents one cell barcode (*i.e.,* droplet containing one or more cells).

a

Flow cytometry

CD14 - BV (y-axis), CD11c - Cy5PE (x-axis)

Monocytes 17%
pDC 10%
mDC 2%

CITE-seq

CD14 [CLR transformed counts] (y-axis), CD11c [CLR transformed counts] (x-axis)

16%
5%
1%

b

Population subset	Marker assayed	Celltype	Flow Cytometry [%]	CITE-Seq [%]
all	CD3+ CD19-	T-cells	52.4	52
	CD3- CD19+	B-cells	13.2	11
	CD14+ CD11c+	Monocytes	16.9	16
	CD14- CD11c++	mDC	1.6	1
	CD14- CD11c+	pDC	10.2	5
CD3+	CD4+ CD8-	CD4 T-cells	70.1	68
	CD4- CD8+	CD8 T-cells	21.9	24
CD3+ CD4+ CD8-	CD2^{dim} CD57-	Naïve CD4 T-cells	64.5	68
	CD2^{bright} CD57-	Memory CD4 T-cells	32.5	30
	CD2^{bright} CD57+	Effector CD4 T-cells	0.8	1
CD3+ CD8+ CD4-	CD2^{dim} CD57-	Naïve CD8 T-cells	38.9	56
	CD2^{bright} CD57-	Memory CD8 T-cells	38	25
	CD2^{bright} CD57+	Effector CD8 T-cells	17.3	14

c

Sorting different populations of CD8 positive cells

All Events — BSC-A (y-axis), FSC-A (x-axis), A: 52.05%

Live/dead sorting — BSC-A (y-axis), DAPI-A-Compensated (x-axis), B: 52.41%, C: 29.05%

CD8 sorting — CD4 APC-A-Compensated (y-axis), CD8 FITC-A-Compensated (x-axis), D: 25.80%, E: 9.05%, F: 18.59%, G: 14.11%

CD8 levels in input — Events (y-axis), CD8 FITC-A-Compensated (x-axis)

CD8+++
CD8++
CD8+
CD8+/-

d

Reanalysis of sorted cells by flow cytometry:

CD8 +++ — E: 0.04%, D: 0.07%, F: 0.07%, G: 98.36% — 2,000 cells

CD8 ++ — E: 0.00%, D: 0.16%, F: 93.34%, G: 0.70% — 2,000 cells

CD8 + — D: 6.79%, E: 74.82%, F: 4.44%, G: 0.00% — 2,000 cells

CD8 +/- — D: 84.84%, E: 1.15%, F: 0.00%, G: 0.00% — 2,000 cells

e

CITE-seq of sorted cells:

CD8 +++ — 442 cells — Density (y-axis), CLR transformed CD8 ADT counts (x-axis)

CD8 ++ — 522 cells — Density (y-axis), CLR transformed CD8 ADT counts (x-axis)

CD8 + — 288 cells — Density (y-axis), CLR transformed CD8 ADT counts (x-axis)

CD8 +/- — 522 cells — Density (y-axis), CLR transformed CD8 ADT counts (x-axis)

Supplementary Figure 3

**Comparing qualitative and quantitative readout in CITE-seq and flow cytometry.**

(a-b) Periperal blood mononuclear cells were processed by flow cytometry and CITE-seq to compare qualitative readout between both technologies. Relevant immune populations were labelled (a) and their abundances relative to the entire population compared (b, see also Fig. 2a,b). (**b**) Relative abundances of relevant immune cell subsets as determined by flow cytometry and CITE-seq (see Fig. 2a,b; and panel a) **(c-e)** Relative quantitative comparison of flow cytometry and CITE-seq. (**c**) Cells were first gated based on forward and side scatter and separated from dead cells. Profile of CD4 and CD8a fluorescence in CBMCs. Colored boxes are gates set to sort different levels of CD8. (**d**) Re-analysis of cells sorted into CD8a very-high (+++), high (++), intermediate (+) and low (+/-) by flow cytometry. Histograms of CD8a levels (fluorescence intensities) in the four different pools of cells. 2,000 cells were measured for each run. **(e)** CD8a levels obtained by CITE-seq of the different pools of cells sorted in panel a. Histograms of four CITE-seq runs of the separate pools. 288-522 cells were measured for each run.
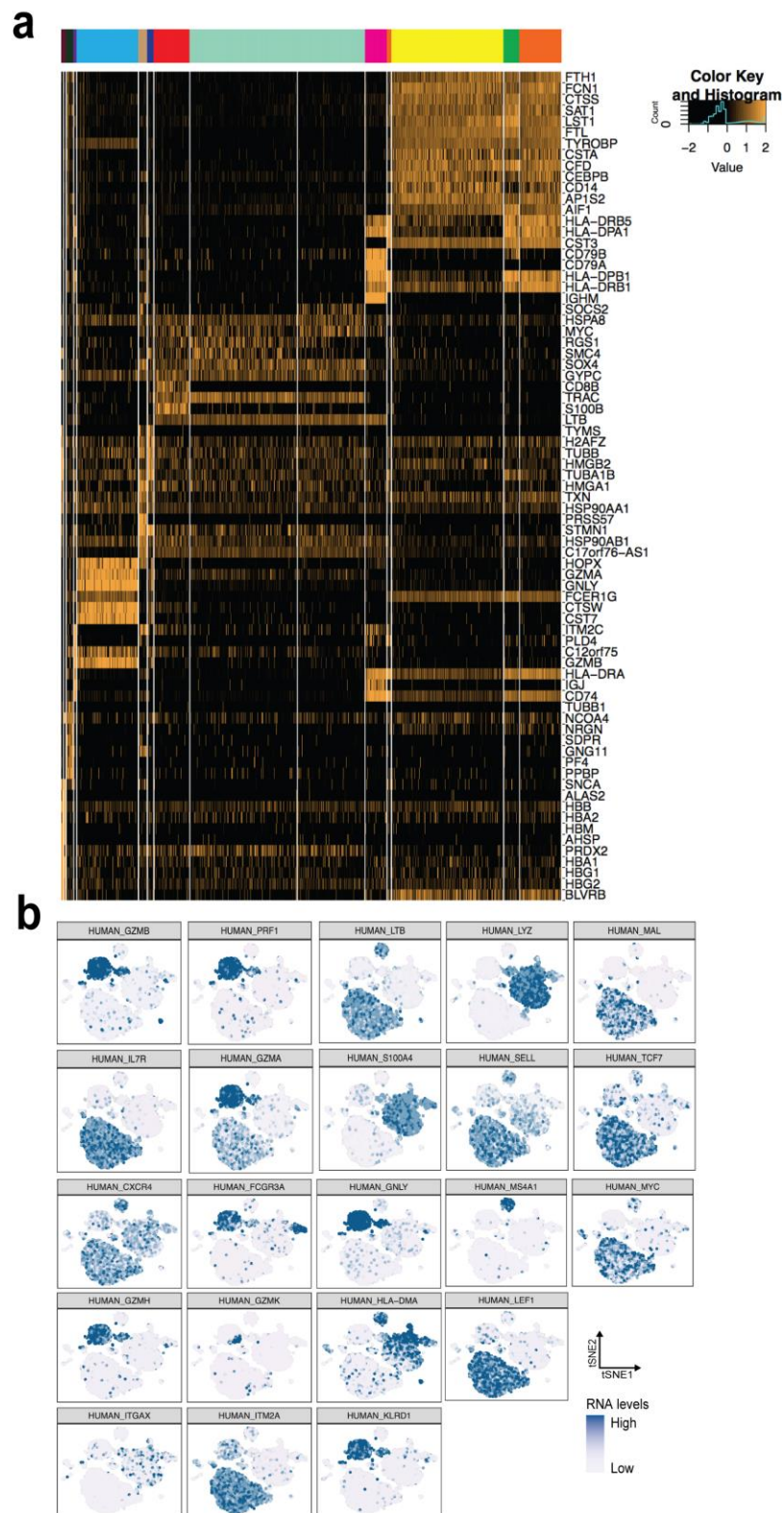
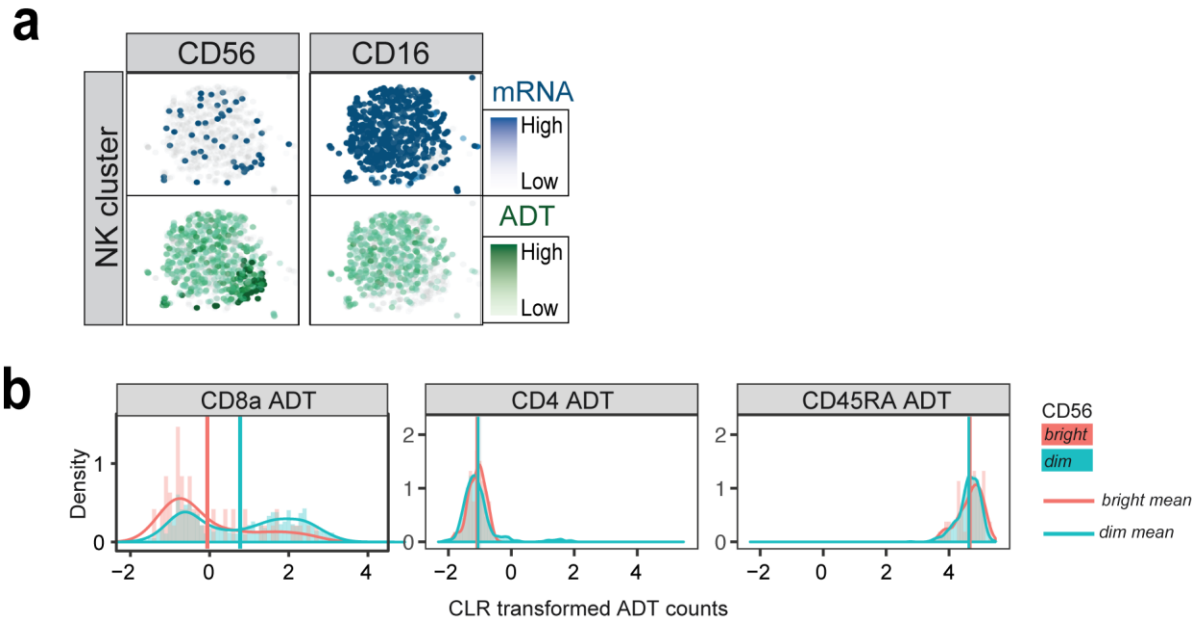**Supplementary Figure 4**

Gene expression in CBMC clusters.

(**a**) Gene expression heatmap of most differentially expressed marker genes defining clusters. Dimensionality reduction followed by modularity optimization was used to cluster 8,005 CBMCs (methods). Cluster color assignments are identical to Figure 3a. The mouse control cell population was excluded from the clustering. (**b**) Expression of individual marker genes in the context of tSNE representation of cell relationships based on single-cell gene-expression profiles. Levels of transcripts corresponding to specific marker genes are indicated by blue shading.
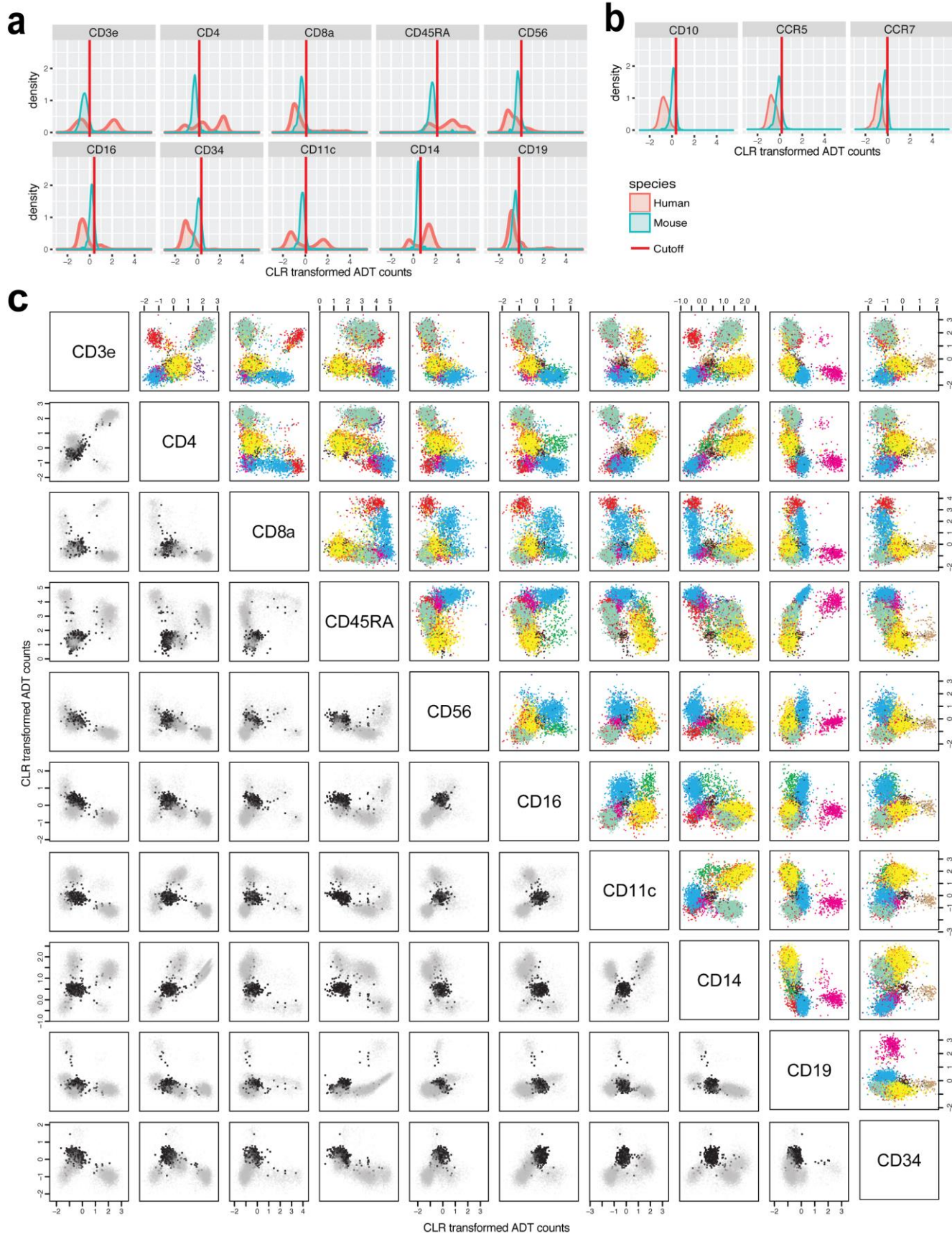
Multimodal bi-axial plots.

(**a**) Histograms of CLR-transformed ADT counts in CBMCs (red) and mouse control cells spiked at very low frequency (blue). Solid line shows the determined cutoff for significant ADT signal (mean of mouse values + standard deviation of mouse values). (**b**) Histograms of CLR-transformed ADT counts for the three antibodies-oligo conjugates in our 13 antibody pool that did not pass the mouse-derived threshold. (**c**) Multimodal bi-axial plots. Pairwise comparison of different CLR-transformed ADT levels in CBMCs. Upper right: CBMCs plotted with colors based on RNA clusters shown in Figure 3a. Lower left: mouse control cells (black) that were spiked at very low frequency are overlaid on the CBMCs (light grey).

Supplementary Figure 6

Joint analysis of protein and RNA to finely resolve NK cell (CD56^{bright} vs CD56^{dim}) populations that have only subtle transcriptomic differences.
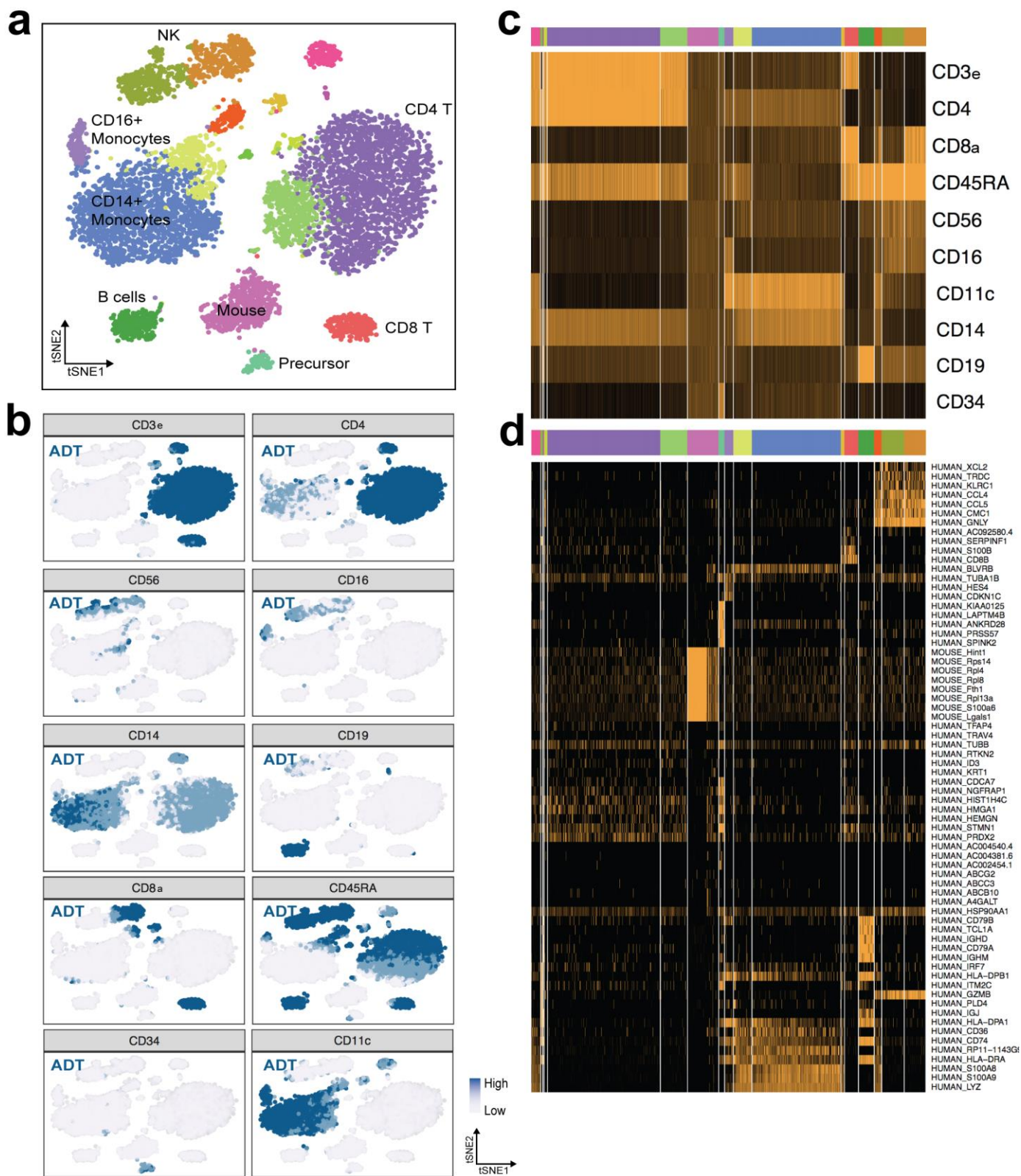
(a) mRNA (blue) and corresponding ADT (green) signal for CD56 and CD16 projected onto the NK cell cluster tSNE plot. Darker shading corresponds to higher levels measured. NK cell cluster was split into CD56^{bright} and CD56^{dim} groups based on CD56 ADT levels. **(b)** Histogram of CD8a levels in the CD56^{bright} and CD56^{dim} cells. Two-sample Kolmogorov–Smirnov test p-value < 0.001 indicates two different CD8a distributions. Histograms for CD4 and CD45RA, ADTs that show low/absent or high expression in these cells, but no difference between CD56^{bright} and CD56^{dim} populations are shown as controls.
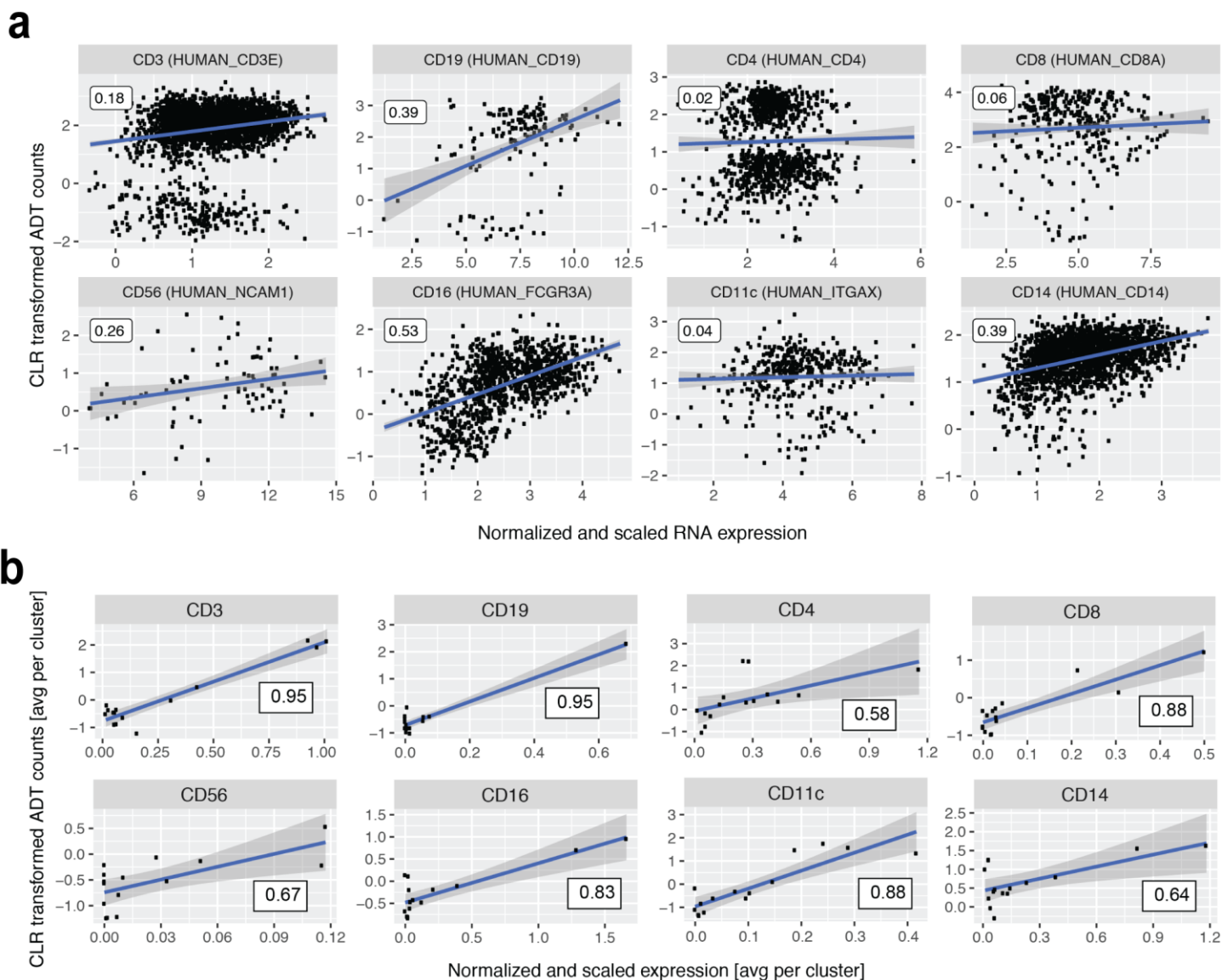
Supplementary Figure 7

Correlations between mRNA and protein marker levels in CITE-seq.

(**a**) Correlation between normalized mRNA expression and CLR-transformed ADT counts at a single cell level. For each gene, cells with no detected mRNA molecules were excluded. Pearson's correlation coefficient is shown in the boxed labels. (**b**) Correlation between normalized mRNA expression and CLR-transformed ADT counts at the cluster level. No cells were excluded. mRNA and ADT signals were averaged per cluster before calculating Pearson's correlation coefficient, shown in boxed labels.

a

NK

CD16+ Monocytes

CD14+ Monocytes

B cells

Mouse

Precursor

CD4 T

CD8 T

tSNE2

tSNE1

b

CD3e — ADT
CD4 — ADT
CD56 — ADT
CD16 — ADT
CD14 — ADT
CD19 — ADT
CD8a — ADT
CD45RA — ADT
CD34 — ADT
CD11c — ADT

High
Low

tSNE2
tSNE1

c

CD3e
CD4
CD8a
CD45RA
CD56
CD16
CD11c
CD14
CD19
CD34

d

HUMAN_XCL2
HUMAN_TRDC
HUMAN_KLRC1
HUMAN_CCL4
HUMAN_CCL5
HUMAN_CMC1
HUMAN_GNLY
HUMAN_AC092580.4
HUMAN_SERPINF1
HUMAN_S100B
HUMAN_CD8B
HUMAN_BLVRB
HUMAN_TUBA1B
HUMAN_HES4
HUMAN_CDKN1C
HUMAN_KIAA0125
HUMAN_LAPTM4B
HUMAN_ANKRD28
HUMAN_PRSS57
HUMAN_SPINK2
MOUSE_Hint1
MOUSE_Rps14
MOUSE_Rpl4
MOUSE_Rpl8
MOUSE_Fth1
MOUSE_Rpl13a
MOUSE_S100a6
MOUSE_Lgals1
HUMAN_TFAP4
HUMAN_TRAV4
HUMAN_TUBB
HUMAN_RTKN2
HUMAN_ID3
HUMAN_KRT1
HUMAN_CDCA7
HUMAN_NGFRAP1
HUMAN_HIST1H4C
HUMAN_HMGA1
HUMAN_HEMGN
HUMAN_STMN1
HUMAN_PRDX2
HUMAN_AC004540.4
HUMAN_AC004381.6
HUMAN_AC002454.1
HUMAN_ABCG2
HUMAN_ABCC3
HUMAN_ABCB10
HUMAN_A4GALT
HUMAN_HSP90AA1
HUMAN_CD79B
HUMAN_TCL1A
HUMAN_IGHD
HUMAN_CD79A
HUMAN_IGHM
HUMAN_IRF7
HUMAN_HLA-DPB1
HUMAN_ITM2C
HUMAN_GZMB
HUMAN_PLD4
HUMAN_IGJ
HUMAN_HLA-DPA1
HUMAN_CD36
HUMAN_CD74
HUMAN_RP11-1143G!
HUMAN_HLA-DRA
HUMAN_S100A8
HUMAN_S100A9
HUMAN_LYZ

Supplementary Figure 8

Clustering of CBMCs based on ADTs.

(**a**) CITE-seq single-cell ADT profiles of ~8,005 CBMCs (and ~600 mouse control cells) were clustered using modularity optimization resulting in 17 cell populations (including the mouse control cell population) with distinct antibody compositions. (**b**) ADT levels for 10 markers in clusters defined by ADT levels. Levels of ADT are indicated by blue to dark blue shading. (**c**) Single-cell ADT level heatmap in the ADT-derived clusters. Colors of clusters in top panel represent colors in panel a. (**d**) Single-cell gene-expression heatmap of top marker genes of ADT-derived clusters. Colors of clusters in top panel represent colors in (a).

Technology or Method	# transcripts	# proteins	# cells	Reference
Droplet based single cell RNA-seq	> 4,000	-	> 10,000	1,2,3
CyTOF	-	< 100	> 10,000	
Flow cytometry / FACS	-	< 30	> 10,000	17
Abseq	-	> 100	> 10,000	22
Index-sorting scRNA-seq	> 4,000	< 30	~ 96 - hundreds	5,6
Wafergen ICELL8	> 4,000	~ 4	~ 1,800	
Fluidigm C1	> 4,000	~ 4	~ 96 - ~ 800	
PLA or PEA & qPCR	~ 96	~ 36	~ 96 - hundreds	11,12,13,14
PLAYR	~ 20	~ 20	> 10,000	15

Supplementary Table 1

Overview of methods that allow multiplexed measurements of RNA and/or proteins in single cells.

Antibody	Reactive	Clone	CITE-seq barcode	Supplier	Note
CD3e	Human	UCHT1	ATCACG	BioLegend, USA	
CD19	Human	HIB19	CGATGT	BioLegend, USA	
CD4	Human	RPA-T4	TGACCA	BioLegend, USA	
CD8a	Human	RPA-T8	GCCAAT	BioLegend, USA	
CD56	Human	MEM-188	CTTGTA	BioLegend, USA	
CD16	Human	B73.1	TTAGGC	BioLegend, USA	
CD11c	Human	B-ly6	TAGCTT	BD Pharmingen, USA	
CCR7	Human	150603	GATCAG	R&D Systems, USA	
CCR5	Human	J418F1	ACTTGA	BioLegend, USA	
CD34	Human	581	GGCTAC	BioLegend, USA	
CD14	Human	M5E2	AGTCAA	BioLegend, USA	
CD10	Human	HI10a	AGTTCC	BioLegend, USA	
CD45RA	Human	HI100	ACAGTG	BioLegend, USA	
CD29	Human	MA1-19105	GCCAAT	Thermo Fisher, USA	used for Human/Mouse experiment only
CD29	Mouse	MA5-16707	CTTGTA	Thermo Fisher, USA	used for Human/Mouse experiment only
CD2	Human	RPA-2.10	GAGTGG	BioLegend, USA	used in quantification validation only
CD57	Human	H-NK1	CGTACG	BioLegend, USA	used in quantification validation only

Supplementary Table 2
List of antibody clones, supplier and barcodes used in this study.